TECHNICAL RESEARCH REPORT

Control of Hysteresis in Smart Actuators with Application to Micro-Positioning

by Xiaobo Tan, John S. Baras, P. S. Krishnaprasad

CDCSS TR 2003-2
(ISR TR 2003-39)

The Center for Dynamics and Control of Smart Structures (CDCSS) is a joint Harvard University, Boston University, University of Maryland center, supported by the Army Research Office under the ODDR&E MURI97 Program Grant No. DAAG55-97-1-0114 (through Harvard University). This document is a technical report in the CDCSS series originating at the University of Maryland.

Web site http://www.isr.umd.edu/CDCSS/cdcss.html

Control of Hysteresis in Smart Actuators with Application to Micro-Positioning

Xiaobo Tan * John S. Baras P. S. Krishnaprasad

Institute for Systems Research and Department of Electrical and Computer Engineering, University of Maryland, College Park, MD 20742 USA

{*xbtan, baras, krishna*}*@isr.umd.edu*

Abstract

Hysteresis in smart material actuators makes the effective use of these actuators quite challenging. The Preisach operator has been widely used to model smart material hysteresis. Motivated by positioning applications of smart actuators, this paper addresses the value inversion problem for a class of discretized Preisach operators, i.e., to find an optimal input trajectory given a desired output value. This problem is solved through optimal state transition of a finite state machine (FSM) that corresponds to the discretized Preisach operator. A state-space reduction scheme for the FSM is developed, which significantly saves the memory and the computation time. As an example, micro-positioning control of a magnetostrictive actuator is investigated. Experimental results are presented to demonstrate the effectiveness of the proposed approach.

Key words: Preisach operator, Inversion, Hysteresis, Magnetostriction, Position control

* Corresponding author.

1 Introduction

Smart materials, such as magnetostrictives, piezoelectrics, electroactive polymers (EAPs) and shape memory alloys (SMAs), all display certain coupling phenomena between applied electro-magnetic/thermal fields and their mechanical/rheological properties. Actuators and sensors made of such materials, often called *smart actuators* and *smart sensors*, have been receiving tremendous interest in the past two decades, due to their broad applications in areas of aerospace, manufacturing, defense, and civil infrastructure systems. However, the hysteretic behavior widely existing in these materials makes their effective use quite challenging. Control of hysteresis in smart materials has attracted attention in recent years [1].

A fundamental idea in coping with hysteresis is to formulate the mathematical model of hysteresis and use inverse compensation to cancel out the hysteretic effect, see, e.g., [2–6]. Hysteresis models can be roughly classified into physics-based models and phenomenological models. The most popular phenomenological hysteresis model used for smart materials has been the Preisach model [7,2,8–10,6,11]. A similar type of operator, called Krasnosel'skii-Pokrovskii (KP) operator has also been used [12,5]. Although in general the Preisach model does not provide physical insight into the problem, it provides a means of developing phenomenological models that are capable of producing behaviors similar to those of physical systems [13].

The inverse compensation approach mentioned above is concerned with the *trajectory* inversion problem: given a desired output trajectory, one computes the corresponding input trajectory whose output trajectory matches the de-

sired one. In many applications like micro-positioning, we are more interested in the following problem: given a desired output *value*, find the input trajectory such that the final value of the output matches the desired value. To distinguish this problem from trajectory inversion, we name it the *value inversion* problem. This problem has been well studied for linear systems (see, e.g., [14] and the references therein), but to our best knowledge, very little has been done in the context of hysteretic systems.

In this paper the value inversion problem for a class of discretized Preisach operators is formulated and solved. Such an operator is represented as a finite state machine (FSM), and the value inversion problem is transformed into a reachability problem for the FSM. The hysteretic dynamics of the FSM is fully characterized, based on which its reachability is proved. Construction of the input sequence for a given state transition is described through an example. Having observed that there may exist a large number of equivalent states for the FSM in practice, we propose a state space reduction scheme, which significantly saves the storage space and the computation time. An algorithm for generating the optimal (the sense of "optimality" will be clear later) representative state in each equivalent class is presented. As an example, we have investigated micro-positioning control of a magnetostrictive actuator. Experimental results have demonstrated the effectiveness of the proposed approach.

The remainder of the paper is organized as follows. Section 2 provides an introduction to the Preisach operator. Section 3 describes the discretization scheme and studies the state reachability problem for the FSM. Section 4 is devoted to the state space reduction scheme. Experimental results are reported in Section 5. Concluding remarks are provided in Section 6 .

2 The Preisach Model

For a pair of thresholds (β, α) with $\beta \leq \alpha$, consider a simple hysteretic element $\hat{\gamma}_{\beta,\alpha}[\cdot,\cdot]$, as illustrated in Fig. 1. For $u \in C([0,T])$ and an initial configuration $\zeta \in \{-1,1\}$, the function

$$v = \hat{\gamma}_{\beta,\alpha}[u,\zeta] : [0,T] \to \{-1,1\}$$

is defined as follows [15]:

$$v(0) \stackrel{\triangle}{=} \begin{cases} -1 & \text{if } u(0) \leq \beta \\ \zeta & \text{if } \beta < u(0) < \alpha \\ 1 & \text{if } u(0) \geq \alpha \end{cases},$$

and for $t \in (0,T]$, setting $X_t \stackrel{\triangle}{=} \{\tau \in (0,t] : u(\tau) = \beta \text{ or } \alpha\}$,

$$v(t) \stackrel{\triangle}{=} \begin{cases} v(0) & \text{if } X_t = \emptyset \\ -1 & \text{if } X_t \neq \emptyset \text{ and } u(\max X_t) = \beta \\ 1 & \text{if } X_t \neq \emptyset \text{ and } u(\max X_t) = \alpha \end{cases}.$$

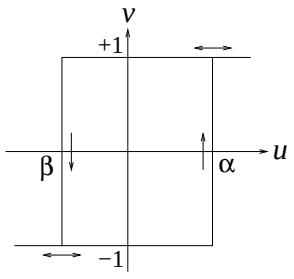

Fig. 1. An elementary Preisach hysteron $\hat{\gamma}_{\beta,\alpha}[\cdot,\cdot]$.

The operator $\hat{\gamma}_{\beta,\alpha}$ is sometimes referred to as an *elementary Preisach hysteron* (we will call it a *hysteron* in this paper), since it is a building block for the

Preisach operator. The Preisach operator is a weighted superposition of all possible hysterons. Define $\mathcal{P}_0 \triangleq \{(\beta, \alpha) \in \mathbb{R}^2 : \beta \leq \alpha\}$. $\mathcal{P}_0$ is called the *Preisach plane*, and each $(\beta, \alpha) \in \mathcal{P}_0$ is identified with the hysteron $\hat{\gamma}_{\beta,\alpha}$. For $u \in C([0, T])$ and a Borel measurable initial configuration ζ_0 of all hysterons:

$$\zeta_0 : \mathcal{P}_0 \to \{-1, 1\},$$

the output of the Preisach operator Γ is defined as

$$y(t) = \Gamma[u, \zeta_0](t) = \int\int_{\mathcal{P}_0} \mu(\beta, \alpha)\hat{\gamma}_{\beta,\alpha}[u, \zeta_0(\beta, \alpha)](t)d\beta d\alpha. \tag{1}$$

The weighting function μ is often referred to as the *Preisach function* [13] or the *density function* [16]. Throughout the paper it is assumed that $\mu \geq 0$. Furthermore, to simplify the discussion, we assume that μ has a compact support, i.e., $\mu(\beta, \alpha) = 0$ if $\beta < \beta_0$ or $\alpha > \alpha_0$ for some β_0, α_0. In this case it suffices to consider the finite triangular area $\mathcal{P} \triangleq \{(\beta, \alpha) \in \mathbb{R}^2 | \alpha \geq \beta, \beta \geq \beta_0, \alpha \leq \alpha_0\}$, as shown in Fig. 2(a). The memory effect of the Preisach operator can be captured by curves in $\mathcal{P}$. At each time instant t, define

$$\mathcal{P}_-(t) \triangleq \{(\beta, \alpha) \in \mathcal{P} | \quad \text{output of } \hat{\gamma}_{\beta,\alpha} \text{ at } t \text{ is} -1\},$$
$$\mathcal{P}_+(t) \triangleq \{(\beta, \alpha) \in \mathcal{P} | \quad \text{output of } \hat{\gamma}_{\beta,\alpha} \text{ at } t \text{ is} +1\},$$

so that $\mathcal{P} = \mathcal{P}_-(t) \cup \mathcal{P}_+(t)$, $\forall t$. Eq. (1) can be rewritten as:

$$y(t) = \int\int_{\mathcal{P}_+(t)} \mu(\beta, \alpha)d\beta d\alpha - \int\int_{\mathcal{P}_-(t)} \mu(\beta, \alpha)d\beta d\alpha. \tag{2}$$

Now assume that at some initial time t_0, the input $u(t_0) = u_0 < \beta_0$. Then the output of every hysteron is -1. Therefore $\mathcal{P}_-(t_0) = \mathcal{P}$, $\mathcal{P}_+(t_0) = \emptyset$ and it corresponds to the "negative saturation" (Fig. 2(b)). Next we assume that the input is monotonically increased to some maximum value at t_1 with $u(t_1) = u_1$. The output of $\hat{\gamma}_{\beta,\alpha}$ is switched to $+1$ as the input $u(t)$ increases past α. Thus at

time t_1, the boundary between $\mathcal{P}_-(t_1)$ and $\mathcal{P}_+(t_1)$ is the horizontal line $\alpha = u_1$ (Fig. 2(c)). Next assume that the input starts to decrease monotonically until it stops at t_2 with $u(t_2) = u_2$. It's easy to see that the output of $\hat{\gamma}_{\beta,\alpha}$ becomes -1 as $u(t)$ sweeps past β, and correspondingly, a vertical line segment $\beta = u_2$ is generated as part of the boundary (Fig. 2(d)). Further input reversals generate additional horizontal or vertical boundary segments.

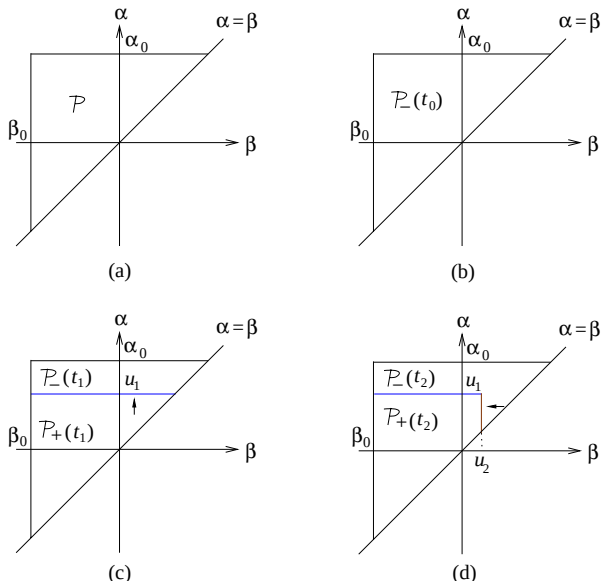

Fig. 2. Memory curves in the Preisach plane.

From the above illustration, one can see that each of $\mathcal{P}_-$ and $\mathcal{P}_+$ is a connected set, and the output of the Preisach operator is determined by the boundary between $\mathcal{P}_-$ and $\mathcal{P}_+$. The boundary is called the *memory curve*. The memory curve has a staircase structure and its intersection with the line $\alpha = \beta$ gives the current input value. The memory curve ψ_0 at $t = 0$ is called the *initial memory curve* and it represents the initial condition of the Preisach operator. Let ζ_{ψ_0} denote the hysteron configuration corresponding to the memory curve ψ_0. In the sequel we will put the initial memory curve ψ_0 as the second argument of Γ, where $\Gamma[\cdot, \psi_0] \triangleq \Gamma[\cdot, \zeta_{\psi_0}]$.

3 The Value Inversion Problem

3.1 The discretized Preisach operator

To use the Preisach operator, one first needs to know the Preisach density. An identification method as well as a review of other identification methods can be found in [6]. Discretization of the Preisach operator is involved in one form or another in any practical identification method and in this paper we will follow the discretization scheme used in [6].

Considering the operating limits of actuators, we assume the input range to be $[u_{min}, u_{max}]$. This range is uniformly discretized into $L+1$ levels. The set of input levels is denoted as $U \triangleq \{u_l, 1 \leq l \leq L+1\}$ with $u_l = u_{min} + (l-1)\delta_u$, where $\delta_u = \frac{u_{max}-u_{min}}{L}$. L will be called the *discretization level* . Input discretization leads to discretization of the Preisach plane. Fig. 3(a) shows the discretization scheme for $L = 3$. The density distribution inside each cell is assumed to concentrate at the cell center (represented by dark dots in Fig. 3(a)) and this results in a discretized Preisach operator, which is now a weighted sum of $\frac{L(L+1)}{2}$ hysterons (see Fig. 4). In Fig. 4, $\nu(\beta_i, \alpha_i)$ denotes the weight for the hysteron $\hat{\gamma}_{\beta_i,\alpha_i}$. Note that although uniform discretization is considered here, the results presented in this paper apply directly to the case of non-uniform discretization.

3.2 The value inversion problem

Since the Preisach operator is rate-independent, and at any time t the memory curve (and thus the output value) depends only on the dominant maximum

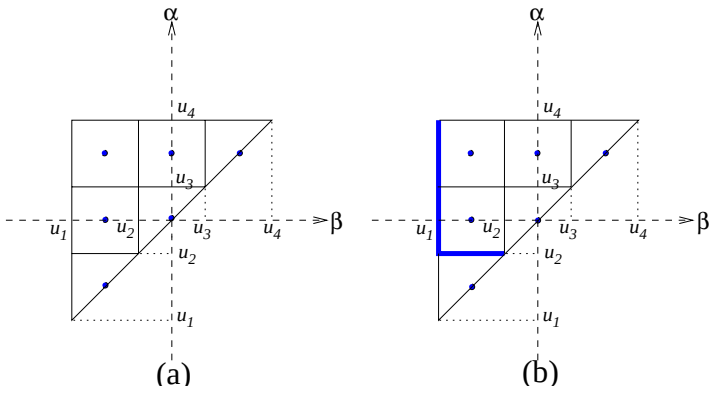

Fig. 3. (a) Discretization of the Preisach plane ($L = 3$); (b) Memory curve "001" (bolded lines).

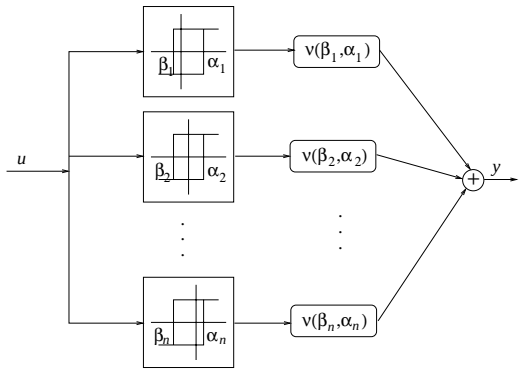

Fig. 4. The discretized Preisach operator.

and minimum values in the past input [13], we restrict ourselves to the discrete time setting and put a sequence instead of a continuous time function as the first argument of Γ.

Let S be the set of input strings taking value in $U = \{u_l, 1 \leq l \leq L+1\}$, i.e., if $s \in S$ is a string of length n, then $s[i] \in U, 1 \leq i \leq n$. To avoid ambiguity, it is tacitly understood that the input is changed monotonically from $s[i]$ to $s[i+1]$. Define S_A to be the set of alternating input strings [16], in the sense that, if $s_a \in S_A$, then $(s_a[i+2] - s_a[i+1])(s_a[i+1] - s_a[i]) < 0,\ \forall i > 0$.

In micro-positioning, one is mainly interested in the final position and cares less about the transient trajectory. This motivates us to study the value in-

version problem for the (discretized) Preisach operator. Let Ψ_d denote the set of memory curves for the discretized Preisach operator. The *value inversion problem* is formulated as: given a desired output value $\overline{y}$ and an initial memory curve $\psi_0 \in \Psi_d$, find $s_a^* \in S_A$, such that

$$|\Gamma_f[s_a^*, \psi_0] - \overline{y}| = \min_{s_a \in S_A} |\Gamma_f[s_a, \psi_0] - \overline{y}|, \tag{3}$$

where $\Gamma_f[s, \psi_0]$ denotes the final value of the output of the Preisach operator under input sequence s; If there is more than one such string achieving (3), find the one with the minimum length.

Remarks:

(1) A discretized Preisach operator is not "onto" since its output takes values in a finite set. Therefore perfect match is not sought in the definition above;

(2) Any $s \in S$ can be *reduced* to some $s_a \in S_A$ using the following rules, starting from $i = 1$: if $(s[i+1] - s[i])(s[i+2] - s[i+1]) \geq 0$, delete $s[i+1]$ and re-index. For example, $s = (u_1, u_3, u_3, u_5, u_4, u_2) \in S$ can be reduced to $s_a = (u_1, u_5, u_2) \in S_A$. The final values of the output under s and s_a are identical (easy to verify). Hence one only needs to search the optimal input sequence in S_A;

(3) The length of an alternating input string is directly linked to the number of input reversals and thus the complexity of implementing that input. Therefore we seek s_a^* with the minimum length.

3.3 The state reachability problem

The discretized Preisach operator is a finite state machine (FSM). Since there are $\frac{L(L+1)}{2}$ hysterons in a discretized Preisach model with discretization level L and each hysteron takes value in $\{-1, 1\}$, the number of states appears to be $2^{L(L+1)/2}$. This is not the case in general, recalling that each of $\mathcal{P}_-$ and $\mathcal{P}_+$ is a connected set (refer to Section 2) and the true state is the memory curve.

Proposition 3.1 *For a discretized Preisach operator with discretization level L, the number of states is 2^L.*

Proof. For a discretized Preisach operator, each memory curve consists of L horizontal or vertical segments of length δ_u, so the total number of memory curves is 2^L. □

The proof motivates an indexing scheme for the memory curve. Starting from the upper left corner, we number each memory curve with L bits corresponding to the L segments: 0 represents vertical, and 1 represents horizontal. For instance, the memory curve represented by the bolded lines in Fig. 3(b) reads "001". To fix the ordering of bits, we refer to the leftmost (rightmost, resp.) bit as bit L (bit 1, resp.).

A complete description for the FSM can now be given. It has state space

$$\Psi_d = \{\psi : \psi = (\alpha^L, \alpha^{L-1}, \cdots, \alpha^1),\ \alpha^j \in \{0, 1\},\ j = 1, \cdots, L\}$$

and input space U. It is a *state output* automaton [17] since the output y of the Preisach operator depends only on the memory curve ψ. Therefore, *the value inversion problem is solved if any state of the FSM is reachable*, because then all we have to do is to find the state whose corresponding output is closest to

the desired value $\bar{y}$.

A state-space representation of a general Preisach operator can be found in [18] and it is shown there that the state space is *approximately reachable*. This "approximate reachability" result was also stated in [13,15] (in a more casual way). As we shall see next, the hysteretic dynamics of a discretized Preisach operator can be characterized elegantly in terms of the FSM. The reachability of the FSM then follows from the characterization.

The state transition function $\Xi_d : \ \Psi_d \times U \rightarrow \Psi_d$ for the FSM can be best described in terms of two state operations, INC: $\Psi_d \rightarrow \Psi_d$ and DEC: $\Psi_d \rightarrow \Psi_d$. For any state $\psi \in \Psi_d$, one can immediately determine the current input $\tilde{u}(\psi)$: $\tilde{u}(\psi) = u_{n+1}$ if ψ contains n "1"s. For $\psi \in \Psi_d$, define

$$INC(\psi) \triangleq \begin{cases} \psi, & \text{if } \tilde{u}(\psi) = u_{L+1} \\ \text{the state after the input is increased by one level,} & \text{if } \tilde{u}(\psi) \neq u_{L+1} \end{cases},$$

and

$$DEC(\psi) \triangleq \begin{cases} \psi, & \text{if } \tilde{u}(\psi) = u_1 \\ \text{the state after the input is decreased by one level,} & \text{if } \tilde{u}(\psi) \neq u_1 \end{cases}.$$

As one can easily verify, INC changes the first "0" bit counting from the right to "1" and leave other bits untouched. A symmetric remark applies to the operation DEC. Therefore bit L (bit 1, resp.) is the most (least, resp.) important bit, in the sense that to switch bit j from 0 (1, resp.) to 1 (0, resp.), one has to first switch all the lower bits to 1 (0, resp.). Fig. 5 illustrates the INC and DEC operations for the case of $L = 3$.

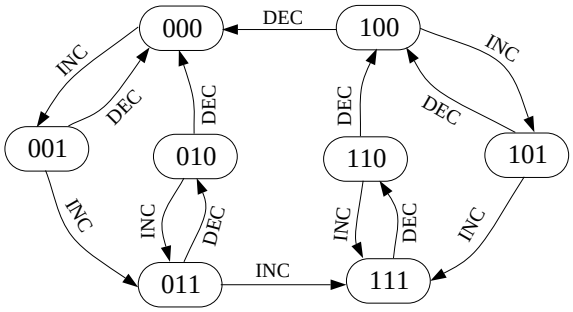

Fig. 5. Operations INC and DEC for $L = 3$.

Given $u \in U$, the state transition function can be expressed as:

$$\Xi_d(\psi, u) = \begin{cases} \psi, \ \text{ if } u - \tilde{u}(\psi) = 0 \\ \underbrace{INC \circ \cdots INC}_{n\ INCs}(\psi), \ \text{if } u - \tilde{u}(\psi) = n\delta_u \\ \underbrace{DEC \circ \cdots DEC}_{n\ DECs}(\psi), \ \text{if } u - \tilde{u}(\psi) = -n\delta_u \end{cases},$$

where "$\circ$" denotes composition of functions.

Proposition 3.2 *Any state is reachable. Let $\psi_i,\ i = 1, 2$, be two states. Let bit n_0 be the leftmost bit at which ψ_1 and ψ_2 differ, and let n_a be the number of alternating bit pairs in ψ_2 from bit n_0 through bit 1. Then ψ_2 is reachable from ψ_1 by applying an input string $s_a^* \in S_A$ of length $n_a + 1$, and the length of any other $s_a \in S_A$ achieving the state transition from ψ_1 to ψ_2 is no less than $n_a + 1$.*

The proposition is a straightforward consequence of the state transition map Ξ_d.

Corollary 3.1 *Any state is reachable from any other state with some $s_a^* \in S_A$ of length no more than L.*

The following example illustrates Proposition 3.2 as well as how to actually construct the input string.

Example 3.1 Assume $L = 5$, $\psi_1 = 00100$, $\psi_2 = 01011$. Then $n_0 = 4$, $n_a = 2$, and the alternating input string s_a^* for achieving the state transition has length 3. The procedure for the state transition is as follows:

- **Step 0.** ψ_1 contains one "1", so the current input value is u_2;
- **Step 1.** Apply u_5 (3 consecutive INCs) to make bit 4 "1" and the state becomes 01111;
- **Step 2.** Apply u_2 (3 consecutive DECs) to make bit 3 "0" and the state becomes 01000;
- **Step 3.** Apply u_4 (2 consecutive INCs) to get ψ_2.

4 A State Space Reduction Scheme

4.1 Reduction of the state space

In general one needs to store the output values of 2^L states for the value inversion problem. For a reasonable discretization level L, this may take lots of memory. In addition, computation cost for sorting and searching these states will be very high. Therefore reducing the number of states without compromising control accuracy is of practical interest.

Two states $\psi_1, \psi_2 \in \Psi_d$ are *equivalent*, denoted as $\psi_1 \equiv \psi_2$, if

$$\Gamma[s, \psi_1] = \Gamma[s, \psi_2], \ \forall s \in S.$$

We call a hysteron in the discretized Preisach operator *non-trivial* if its asso-

ciated weight is not zero, and *trivial* otherwise. Existence of trivial hysterons leads to equivalent states. This is illustrated in Fig. 6(a), where the hysterons marked with "•"(and labeled by $\gamma_1, \cdots, \gamma_5$) are assumed to be non-trivial and those marked with "○" are assumed to be trivial. It's easy to verify that the following states in Fig. 6(a) are equivalent: 0101, 0110, 1001 and 1010. From the experimental result of measure identification (see Fig. 10), we see that indeed many hysterons carry weights of zero or close to zero, and this provides room for the state space reduction.

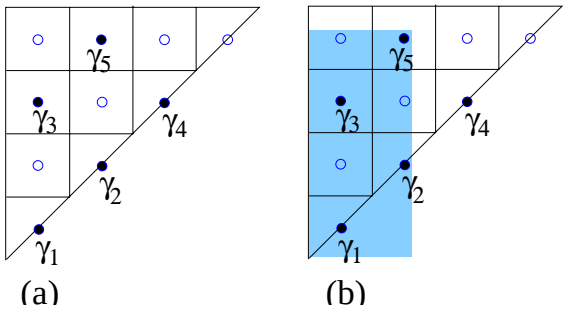

Fig. 6. (a) Existence of equivalent states ($L = 4$); (b) Illustration of the shaded set.

The original state space Ψ_d is thus a disjoint union of equivalent classes of states. Ψ_d can be reduced, so that in the reduced state space $\widetilde{\Psi}$ each element is an equivalent class in Ψ_d, i.e., $\widetilde{\Psi} = \Psi_d/\equiv$. Denote the set of non-trivial hysterons as $\mathcal{N}$, i.e., $\mathcal{N} \stackrel{\triangle}{=} \{\hat{\gamma}_{\beta,\alpha} : \nu_{\beta,\alpha} > 0\}$, where $\nu_{\beta,\alpha}$ is the weight of $\hat{\gamma}_{\beta,\alpha}$. For $\psi \in \Psi_d$, define $\mathcal{S}(\psi)$ to be the set of non-trivial hysterons underneath the memory curve corresponding to ψ. From the example above, we can see that $\psi_1 \equiv \psi_2$ if and only if $\mathcal{S}(\psi_1) = \mathcal{S}(\psi_2)$. Therefore, a member of $\widetilde{\Psi}$ can be identified with a subset $\tilde{\psi}$ of $\mathcal{N}$ that satisfies the following condition: there exists $\psi \in \Psi_d$, such that $\tilde{\psi} = \mathcal{S}(\psi)$. To better capture the latter property, we introduce the notion of a *Lower-Left-Shaded Set* . The Lower-Left-Shaded Set (abbreviated as the shaded set hereafter) $\mathcal{A}(\hat{\gamma}_{\beta,\alpha})$ of a hysteron $\hat{\gamma}_{\beta,\alpha} \in \mathcal{N}$ is

defined to be

$$\mathcal{A}(\hat{\gamma}_{\beta,\alpha}) = \{\hat{\gamma}_{\beta',\alpha'} \in \mathcal{N} : \ \hat{\gamma}_{\beta',\alpha'} \neq \hat{\gamma}_{\beta,\alpha}, \beta' \leq \beta, \alpha' \leq \alpha\}.$$

The geometric interpretation of the shaded set of $\hat{\gamma}_{\beta,\alpha}$ is clear: imagining two rays from $\hat{\gamma}_{\beta,\alpha}$ in the Preisach plane, one pointing downwards and the other to the left, the shaded set consists of non-trivial hysterons lying between the two rays. For example, in Fig. 6(b), $\mathcal{A}(\gamma_5) = \{\gamma_1, \gamma_2, \gamma_3\}$. If $\hat{\gamma}_{\beta,\alpha}$ lies underneath some memory curve ψ', it follows from analysis of the Preisach plane that all elements of $\mathcal{A}(\hat{\gamma}_{\beta,\alpha})$ must also lie underneath ψ'. Therefore we conclude that $\tilde{\psi} \subset \mathcal{N}$ is identified with a member of $\widetilde{\Psi}$ if and only if the following holds:

$$\mathcal{A}(\hat{\gamma}_{\beta,\alpha}) \subset \tilde{\psi} \ , \forall \, \hat{\gamma}_{\beta,\alpha} \in \ \tilde{\psi}. \tag{4}$$

To ease presentation, from now on we will simply write $\tilde{\psi} \in \widetilde{\Psi}$ if (4) is satisfied. One can now list all members in $\widetilde{\Psi}$ using a tree-structured algorithm:

- **Step 1.** List the equivalent class having no non-trivial hysterons (negative saturation);
- **Step 2.** List equivalent classes with one constituent non-trivial hysteron, i.e., the shaded set of every such hysteron is empty;
- **Step 3.** Starting from each equivalent class (*parent class*) $\tilde{\psi}$ with n non-trivial hysterons, we list equivalent classes (*children classes*) with $n+1$ non-trivial hysterons by finding another hysteron $\hat{\gamma} \in \mathcal{N}$ such that:
  - $\hat{\gamma}$ is not included in $\tilde{\psi}$,
  - $\mathcal{A}(\hat{\gamma}) \subset \tilde{\psi}$, i.e., $\tilde{\psi} \cup \hat{\gamma}$ is an eligible member of $\widetilde{\Psi}$, and
  - $\tilde{\psi} \cup \hat{\gamma}$ does not coincide with any other equivalent class $\tilde{\psi}'$ with $n+1$ constituent hysterons that has been listed so far;
- **Step 4.** Continue Step 3 until $\tilde{\psi} = \mathcal{N}$ (positive saturation) is listed.

The equivalent classes are sorted according to their output values during the above enumeration process. One can save computation time by using the fact that the output of a child class is always greater than that of its parent.

4.2 Generation of best representative states

For the purpose of realizing state transition, one needs to find a representative state $\psi \in \Psi_d$, i.e., a memory curve, for every $\tilde{\psi} \in \widetilde{\Psi}$. From Proposition 3.2, the number of alternating bit pairs of a state ψ is closely related to the number of input reversals required for the state transition. Therefore the best representative state $\psi^* \in \Psi_d$ for $\tilde{\psi} \in \widetilde{\Psi}$ should have the least number of alternating bit pairs among all states in the equivalent class $\tilde{\psi}$.

An algorithm is developed here to generate the optimal representative ψ^* for $\tilde{\psi} \in \widetilde{\Psi}$. We first draw two candidate memory curves $\psi^*_{\downarrow}$ and $\psi^*_{\rightarrow}$, and then pick ψ^* to be the one whose number of alternating bit pairs is less. When growing a memory curve starting from the left upper corner of the discretized Preisach plane, one has two possible directions for each segment of the curve: going downwards (denoted as "$\downarrow$") or going to the right (denoted as "$\rightarrow$"). The candidate $\psi^*_{\downarrow}$ is obtained as follows: start with "$\downarrow$" and continue that direction as long as it is feasible to do so (i.e., no constituent hysteron of $\tilde{\psi}$ is left out); when it is infeasible to continue "$\downarrow$", switch to "$\rightarrow$" and keep going with that direction until it is infeasible for $\tilde{\psi}$ (i.e., non-constituent hysterons will be included). Continue with these rules until all L segments are drawn. Similarly one obtains $\psi^*_{\rightarrow}$ by starting with "$\rightarrow$". Note that "$\rightarrow$" is feasible whenever "$\downarrow$" is not, and vice versa.

Proposition 4.1 *The representative ψ^* obtained in the above scheme has the least number of alternating bit pairs among all states in the equivalent class $\tilde{\psi}$.*

Proof. For any state $\psi \in \tilde{\psi}$ starting with "$\downarrow$", one can show its number of alternating bit pairs is no less than that of $\psi^*_{\downarrow}$ by exploiting the strategy in generating $\psi^*_{\downarrow}$.

Instead of giving a general proof, we will illustrate the essential idea by looking at a concrete example with discretization level $L = 8$ (Fig. 7). Assume that the memory curve represented by the bolded lines A-B-C-D-E ("00111001") is $\psi^*_{\downarrow}$. Let ψ be any other state in the same equivalent class $\tilde{\psi}$ starting with "$\downarrow$". Now imagine we are growing the two curves $\psi^*_{\downarrow}$ and ψ segment by segment, starting from the left upper corner. The curve ψ has to switch to "$\rightarrow$" no later than it reaches the point B (since otherwise it will be infeasible). This implies that when the first alternating bit pair in $\psi^*_{\rightarrow}$ occurs, at least one alternating bit pair has occured in ψ. For the same reason, ψ has to switch to "$\downarrow$" before $\psi^*_{\downarrow}$ does so at point C. This argument goes on until the line $\alpha = \beta$ is hit and the drawing is completed. Hence the number of alternating bit pairs in ψ is no less than that in $\psi^*_{\downarrow}$. The curve represented by the dashed lines A-F-G-H-I-E in Fig. 7 gives an example of such ψ.

Analogously for any state ψ starting with "$\rightarrow$", one can show its number of alternating bit pairs is no less than that of $\psi^*_{\rightarrow}$. The proof is now complete. □

Example 4.1 For the equivalent class $\{\gamma_1, \gamma_2, \gamma_3\}$ in Fig. 6(a), $\psi^*_{\downarrow} = 0110$ with 2 alternating bit pairs and $\psi^*_{\rightarrow} = 1001$ with the same number of alternating bit pairs. So $\psi^* = \psi^*_{\downarrow}$ (or $\psi^*_{\rightarrow}$).

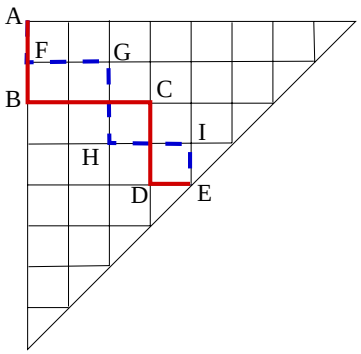

Fig. 7. Illustration of the proof of Proposition 4.1.

5 Experimental Results

In this section the value inversion approach together with the state space reduction scheme is applied to micro-positioning control of a magnetostrictive actuator. Magnetostriction is the phenomenon of strong coupling between magnetic properties and mechanical properties of some ferromagnetic materials (e.g., Terfenol-D): strains are generated in response to an applied magnetic field, while conversely, mechanical stresses in the materials produce measurable changes in magnetization. Fig. 8 shows a sectional view of a Terfenol-D actuator manufactured by ETREMA Products, Inc. By varying the current in the coil, one varies the magnetic field in the Terfenol-D rod and thus controls the displacement of the rod head. Fig. 9 displays the hysteresis in the magnetostrictive actuator.

When operated in a low frequency range (typically below 5 Hz), the displacement y can be related to the bulk magnetization M by a square law $\lambda = a_1 M^2$ for some constant $a_1 > 0$ [19], and the input current I can be related to the magnetic field H (assumed uniform) along the rod direction by a proportional law: $H = c_0 I$, where c_0 is the coil factor. Then the magnetostrictive hysteresis between y and I is fully captured by the ferromagnetic hysteresis between

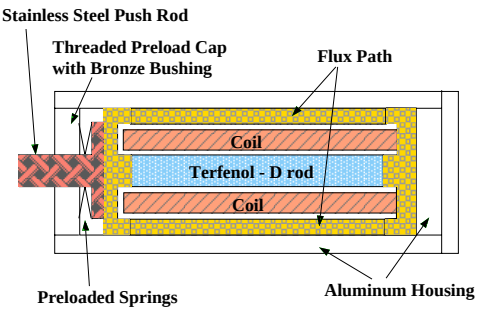

Fig. 8. Sectional view of the Terfenol-D actuator [19](Original source: Etrema Products Inc.).

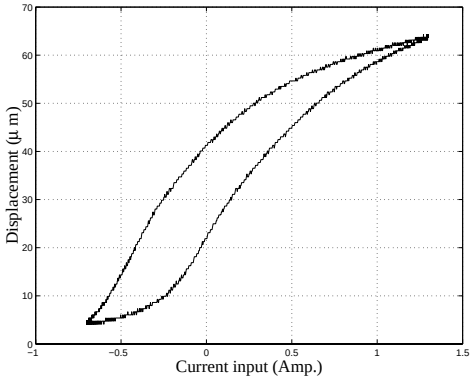

Fig. 9. Hysteresis in the magnetostrictive actuator

M and H, which is modeled by the Preisach operator. The Preisach plane is discretized with $L = 25$ which results in 300 hysterons. Fig. 10 displays the Preisach weighting masses identified through a least squares algorithm [6]. By treating 201 hysterons whose weights are zero or very small as trivial, we are left with 99 nontrivial hysterons. The final number of states in the reduced state space is 99,217 compared to 33,554,432 in the original state space.

Our experimental setup is as shown in Fig. 11. The displacement of the actuator is measured with a LVDT sensor, which has a precision of about 1 μm. DSpace ControlDesk is used to send control commands and collect data.

Given a sequence of 8 desired displacement values (10 μm, 30 μm, 15 μm, 40 μm, 20 μm, 40 μm, 60 μm and 50 μm),the control objective is to drive

mo

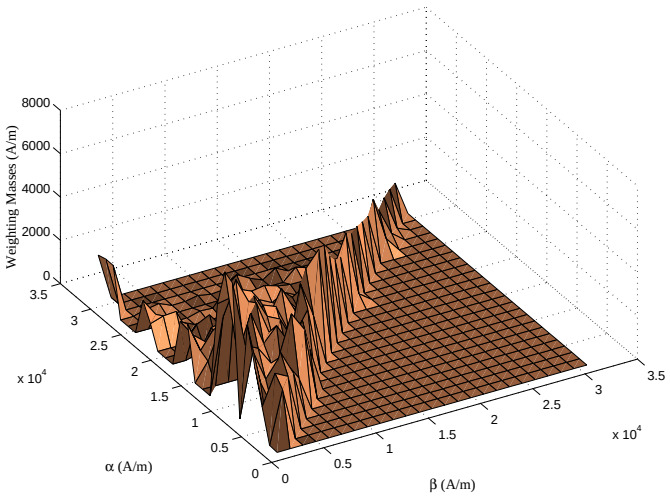

Fig. 10. Distribution of the Preisach weighting masses (L=25).

the actuator head to these positions consecutively. Three control schemes are implemented to achieve the positioning goal. The first one is based on the value inversion scheme, the second is based on the closest match algorithm for trajectory inversion (see [6]), and the third scheme is based on a non-hysteretic model where the input-output relationship is approximated by a single-valued function $y = -7.44I^3 - 2.63I^2 + 40.81I + 30.34$. The trajectories of the current input and the measured displacement under these schemes are shown in Fig. 12 through Fig. 14. For presentation purposes, we intentionally hold the input current constant for about 1 second after each positioning is completed. Fig. 15 compares the errors of the three schemes for the eight positioning tasks. It can be seen that Scheme 1 yields the minimum positioning error. As a trajectory inversion algorithm, Scheme 2 does not allow input reversals for each desired output value and thus has less control freedom than Scheme 1 does. This explains why scheme 1 is better than scheme 2. Scheme 3 delivers the worst performance because hysteresis is not taken into account.

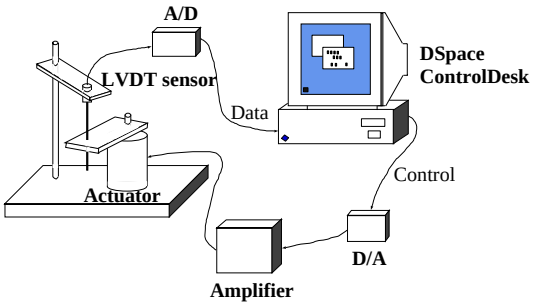

Fig. 11. Experimental setup.

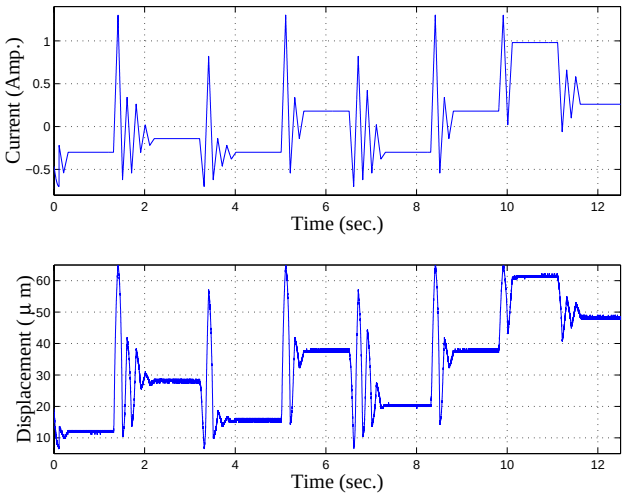

Fig. 12. Micro-positioning control based on the value inversion scheme.

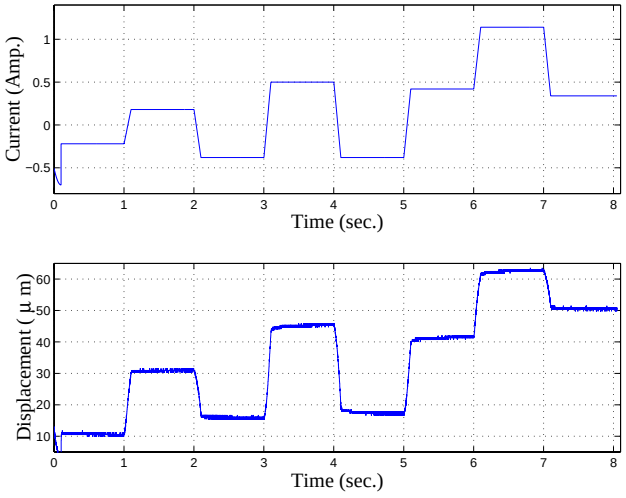

Fig. 13. Micro-positioning control based on the closest match algorithm.

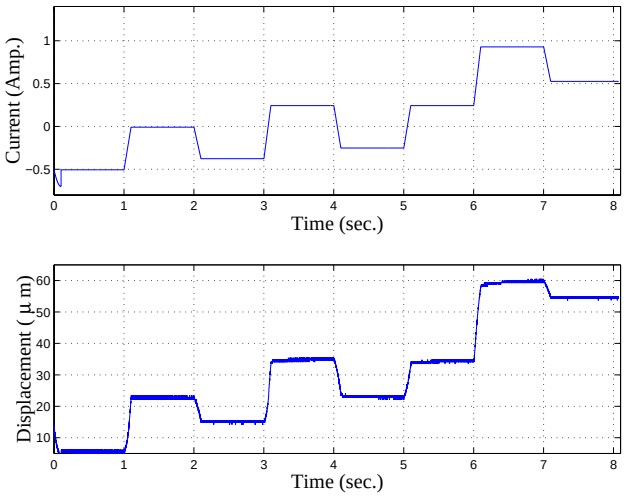

Fig. 14. Micro-positioning control based on a non-hysteretic model.

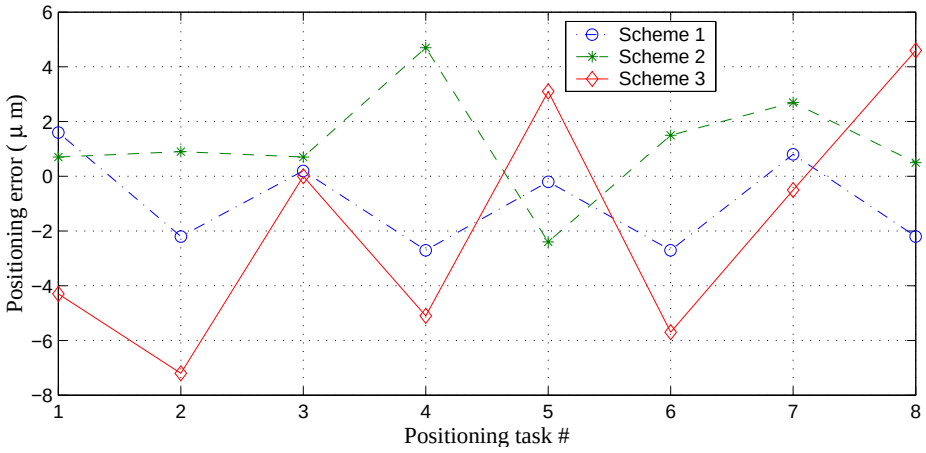

Fig. 15. Comparison of three schemes. Scheme 1: the value inversion algorithm; Scheme 2: the closest match algorithm; Scheme 3: the inversion algorithm based on a non-hysteretic model.

6 Conclusions

In this paper a novel type of inversion problem, called the value inversion problem, for a class of discretized hysteresis operators has been studied. Unlike most inversion problems discussed in the literature on hysteresis control, the value inversion problem is to find an optimal input trajectory given a desired value of the hysteresis output. This problem was motivated by positioning

applications of smart actuators.

The Preisach operator has been used for the modeling of hysteresis. When discretized, it can be represented by a FSM. Based on a concise indexing scheme for the memory curve, the dynamics of the FSM is captured by simple rules. The original value inversion problem was converted to a state reachability problem of the FSM. Implementation of state transitions were illustrated through examples. The notion of state space reduction was developed for a discretized Preisach operator, and algorithms for generating the reduced state space and for constructing the optimal representative state were also presented. This approach has been applied to micro-positioning control of a magnetostrictive actuator and its effectiveness has been demonstrated through comparison with two other inversion schemes.

Acknowledgment

This research was supported by the Army Research Office under the ODDR&E MURI97 Program Grant No. DAAG55-97-1-0114 to the Center for Dynamics and Control of Smart Structures (through Harvard University).

References

[1] S. O. R. Moheimani, G. C. Goodwin, Guest editorial introduction to the special issue on dynamics and control of smart structures, IEEE Transactions on Control System Technology 9 (1) (2001) 3–4.

[2] D. Hughes, J. T. Wen, Preisach modeling and compensation for smart material hysteresis, in: Active Materials and Smart Structures, Vol. 2427 of SPIE, 1994, pp. 50–64.

[3] G. Tao, P. V. Kokotović, Adaptive control of plants with unkown hystereses, IEEE Transactions on Automatic Control 40 (2) (1995) 200–212.

[4] R. C. Smith, Inverse compensation for hysteresis in magnetostrictive transducers, CRSC Technical Report, North Carolina State University (CRSC-TR98-36).

[5] W. S. Galinaitis, R. C. Rogers, Control of a hysteretic actuator using inverse hysteresis compensation, in: V. Varadan (Ed.), Mathematics and Control in Smart Structures, Vol. 3323 of SPIE, 1998, pp. 267–277.

[6] X. Tan, R. Venkataraman, P. S. Krishnaprasad, Control of hysteresis: theory and experimental results, in: V. S. Rao (Ed.), Modeling, Signal Processing, and Control in Smart Structures, Vol. 4326 of SPIE, 2001, pp. 101–112.

[7] A. A. Adly, I. D. Mayeygoyz, A. Bergqvist, Preisach modeling of magnetostrictive hysteresis, Journal of Applied Physics 69 (8) (1991) 5777–5779.

[8] J. Schäfer, H. Janocha, Compensation of hysteresis in solid-state actuators, Sensors and Actuators A 49 (1-2) (1995) 97–102.

[9] P. Ge, M. Jouaneh, Tracking control of a piezoceramic actuator, IEEE Transactions on Control Systems Technology 4 (3) (1996) 209–216.

[10] R. B. Gorbet, D. W. L. Wang, K. A. Morris, Preisach model identification of a two-wire SMA actuator, in: Proceedings of IEEE International Conference on Robotics and Automation, 1998, pp. 2161–2167.

[11] D. Croft, G. Shed, S. Devasia, Creep, hysteresis, and vibration compensation for piezoactuators: atomic force microscopy application, Journal of Dynamic Systems, Measurement, and Control 123 (1) (2001) 35–43.

[12] H. T. Banks, A. J. Kurdila, G. Webb, Identification of hysteretic control influence operators representing smart actuators, Part I: Formulation, Mathematical Problems in Engineering 3 (4) (1997) 287–328.

[13] I. D. Mayergoyz, Mathematical Models of Hysteresis, Springer Verlag, New York, 1991.

[14] H. Perez, S. Devasia, Optimal output-transitions for linear systems, Automatica 39 (2) (2003) 181–192.

[15] A. Visintin, Differential Models of Hysteresis, Springer, 1994.

[16] M. Brokate, J. Sprekels, Hysteresis and Phase Transitions, Springer Verlag, New York, 1996.

[17] L. S. Bobrow, M. A. Arbib, Discrete Mathematics: Applied Algebra for Computer and Information Science, W. B. Saunders Company, 1974.

[18] R. B. Gorbet, K. A. Morris, D. W. L. Wang, Control of hysteretic systems: a state-space approach, in: Y. Yamamoto, S. Hara (Eds.), Learning, Control and Hybrid Systems, Vol. 241 of Lecture Notes in Control and Information Sciences, Springer, New York, 1998, pp. 432–451.

[19] R. Venkataraman, Modeling and adaptive control of magnetostrictive actuators, Ph.D. thesis, University of Maryland, College Park (1999).